

Green Synthesis and Characterization of Zinc Oxide Nanoparticles using *Plectranthus amboinicus* Leaf Extract

P. Srisathya¹ and R. Radhika^{2*}

¹M. Sc., Physics, Vellalar College for Women, Erode - 638012, Tamil Nadu, India

²Assistant Professor, Department of Physics, Vellalar College for Women, Erode - 638012, Tamil Nadu, India;

radhikamsc88@gmail.com

Abstract

Nanoscience and nanotechnology have been established recently a new interdisciplinary science and now a day it is one of the most attractive research area in modern material science. The aim of this work was to investigate the photo catalytic property of Zinc oxide nano particles by using *Plectranthus amboinicus* leaf extract at various concentration. The average crystalline size of the prepared ZnO nanoparticles was calculated in XRD analysis. The UV-visible absorption spectrum indicates the band gap of green synthesis ZnO nanoparticles. The synthesized zinc oxide nanoparticles were subjected to Fourier Transform Infrared spectroscopy (FTIR) analysis to detect the various functional groups associated with the prepared nano particles. The Scanning Electron Microscopy (SEM) analysis to measure the morphological structure of synthesized ZnO Nano particles. Moreover, the green synthesized ZnO nanoparticles showed a superior photo catalytic performance than chemically synthesized ZnO particles.

Keyword: *Plectranthus amboinicus*, Photocatalytic Effect, SEM, UV, XRD, ZnO.

1. Introduction

Nanotechnology stands as a pivotal domain with significant implications for the advancement of both science and medicine. In the contemporary landscape, substantial attention is directed towards the investigation of metal oxide Nanoparticles (NPs), given their notable appeal in electronics and medical applications due to their easy accessibility, straightforward preparation methods, and established human safety profiles at known concentrations¹. The synthesis of NPs encompasses a range of techniques, involving both physicochemical and biological routes. Of these, the “green chemistry” approach has garnered considerable interest, primarily due to its cost-effective and environmentally conscious attributes^{2,3}.

Among the various metal oxide NPs, Zinc Oxide (ZnO) enjoys wide utilization attributed to its expansive surface area, remarkable catalytic prowess, chemical

stability, efficient absorption capabilities, substantial band gap (3.37 eV), compatibility with living systems, and cost-effectiveness. These ZnO NPs find diverse applications spanning gas sensors, luminescent textiles, optoelectronics, biosensors, solar cells, photodetectors, photocatalysis, antibacterial functions, and catalytic roles. Presently, strategies revolving around photo-excited bacteria extermination and related light-responsive materials are gaining prominence due to their swift and potent antibacterial effects. It has been previously noted that ZnO NPs synthesized through environmentally friendly means exhibit more robust antimicrobial and antifungal attributes compared to conventionally produced NPs⁴⁻⁷. Furthermore, ZnO NPs possess a commendable safety profile for human use and offer multifaceted medicinal applications such as carriers for antioxidants, wound healing facilitators, agents against cancer and atherosclerosis.

*Author for correspondence

Plectranthus amboinicus, commonly known as Indian borage or Mexican mint, is a medicinal and aromatic plant known for its various biological activities and potential applications. ZnO (Zinc Oxide) nanoparticles are semiconductor nanomaterials that exhibit excellent photocatalytic properties, meaning they can facilitate chemical reactions using light energy⁸⁻¹⁰. When combined, *Plectranthus amboinicus* mediated ZnO nanoparticles could have interesting applications in photocatalytic studies^{11,12}. ZnO nanoparticles are known for their excellent photocatalytic activity. They can absorb photons and generate electron-hole pairs, which can then participate in various redox reactions. The addition of *Plectranthus amboinicus* compounds during the synthesis process might enhance the photocatalytic activity of ZnO nanoparticles. The phytochemicals could act as sensitizers, improving the absorption of light and increasing the efficiency of electron-hole pair generation¹³⁻¹⁵.

Plectranthus amboinicus is known to contain a variety of phytochemicals, such as monoterpeneoids, diterpeneoids, triterpeneoids, sesquiterpeneoids, phenolics, flavonoids, and esters. In this study, we introduced a novel approach by utilizing different ratios of *Plectranthus amboinicus* leaf extract. These pigments are believed to serve as both reducing and capping agents in the eco-friendly synthesis of spherical ZnO nanoparticles. This method allows for precise control over particle size and enhances their photocatalytic properties.

2. Experimental Procedure

2.1 Materials

Plectranthus amboinicus leaves are collected from erode nearest agriculture land. Zinc acetate dihydrate $Zn(CH_3COO)_2 \cdot 2H_2O$, sodium hydroxide (NaOH) and Distilled water are used without extra purification.

2.2 Preparation of Leaf Extract

Freshly collected *Plectranthus amboinicus* leaves were washed thoroughly with distilled water to remove the dust particles. The washed leaves are dried at room temperature. After that 10g of *Plectranthus amboinicus* cut into small pieces and it was mixed with 60ml of distilled water then boiled at 100°C for 30 minutes. After 24 hours, the solution was filtered using Whatman filter paper. This *Plectranthus amboinicus* leaf extract was used in ZnO preparation.

2.3 Synthesis of ZnO Nanoparticles

In ZnO preparation, 10g of $Zn(CH_3COO)_2 \cdot 2H_2O$ dissolved in 100ml water and stirring at 500RPM for 15 minutes. Then 5g of NaOH dissolved in 100ml of water and added drop wise. This mixture was kept continuous stirring for two hours during a magnetic stirrer under 800RPM level. Aqueous *Plectranthus amboinicus* leaf extract was added 10 drops is labelled as ZnOp-1 then added 20 drops of *Plectranthus amboinicus* leaf extract is labelled as ZnOp-2 respectively. The P^H value of the prepared nanoparticles was maintaining in the range of 6-7. The precipitate was collected and dried in an oven at 100°C half an hour. The prepared white powder was kept at 150°C for two hours in muffle furnace. Figure 1 shows a schematic diagram representing the process of ZnO nanoparticle preparation.

3. Result and Discussion

3.1 XRD Analysis

Figure 2 shows the XRD pattern gives the structural properties of prepared ZnO nanoparticles. The diffractogram shows the intensity of the diffracted rays as a function of diffraction angles, corresponding to the angles $31.84^\circ, 36.27^\circ, 47.55^\circ, 56.62^\circ, 62.91^\circ, 66.39^\circ, 68.02^\circ, 69.13^\circ$ corresponding to the lattice planes (100), (002), (101), (102), (110), (103), (200), (112), (201) respectively. Those observed peaks are in good agreement with those for hexagonal ZnO wurtzite structure. The average crystalline size (D) of the nanoparticles was measured using the Debye-Scherrer formula,

$$D = K \lambda / \beta \cos \theta \text{ A}^\circ$$

Where, D is the average crystalline size. K is the shape factor of scherers constant (0.9), λ is the wave length of X ray 1.5406 A° , β is the full width at half maximum (rad), and θ is the Braggs diffraction angle (degree). Using Scherer's formula, the average size of the nanoparticles of pure zinc oxide is 32.6nm. The average crystalline size of *Plectranthus amboinicus* mediated zinc oxide nanoparticles is 30.7nm, 27.7nm for ZnOp-1, ZnOp-2 respectively. The characteristics peaks of the synthesized Nano particles are completely identical to those from the JCPDS data (36-1451). If the ratio of the *Plectranthus amboinicus* leaf extracts increased, the average crystalline size was decreased. Because the crystalline size reduction leads to the contraction of bond length between the surface and the atom¹⁶.

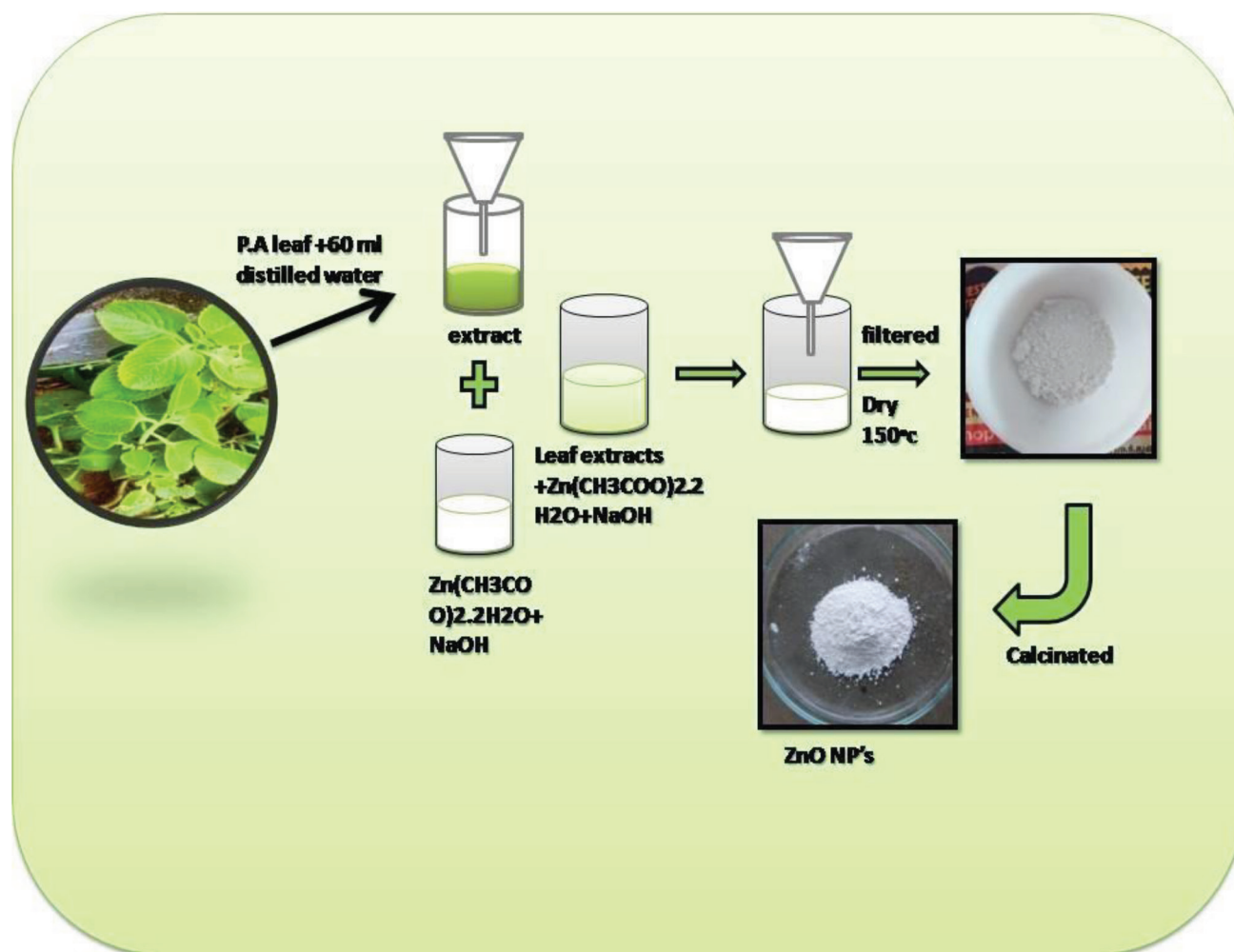


Figure 1. Schematic Diagram Preparation of ZnO Nanoparticles.

3.2 FTIR Analysis

Figure 3 represents FTIR spectra of the synthesized ZnO nanoparticles in the range of 400 cm to 4000 cm. The functional groups were responsible for reducing zinc ions to ZnO, which was observed as bands. Each of the bands corresponding in stretching mode 3329 - 3384 cm corresponding to O-H stretching of phenolic compound. The sharp band at 555 cm is attributed to the presence of ZnO stretching mode. The multiple bands between 1000 - 1700 represent C-O stretching of esters and carboxylic functional group¹⁷.

3.3 SEM Analysis

The morphological structure of green synthesized ZnOp-1, ZnOp-2 and chemical synthesized ZnO NP's were characterized by Scanning Electron Microscopic analysis. Figure 4 shows that the SEM images of synthesized NP's

with different magnification. It can be observed that the synthesized ZnO NP's is spherical in shape, other green synthesized ZnOp-1, and ZnOp-2 are rod in structure. The particle size of the bio synthesized ZnOp-1, ZnOp-2 NP's is varying between 90-112 nm in Figure 5.

The SEM image of pure zinc oxide nanoparticles are much cleared spherical shape and uniformly distributed. In this image the particles have high surface area so they can agglomerate. In order to avoid this agglomeration and unwanted growth along with capping and stabilizing agent. Here the *Plectranthus amboinicus* leaf extract act as capping and reducing agent and it determines the shape and size of the nanoparticles¹⁸⁻²⁰.

3.4 EDX

Figures 6-8 shows EDX spectra of prepared ZnO nanoparticles. EDX revealed a high signal for Zinc and

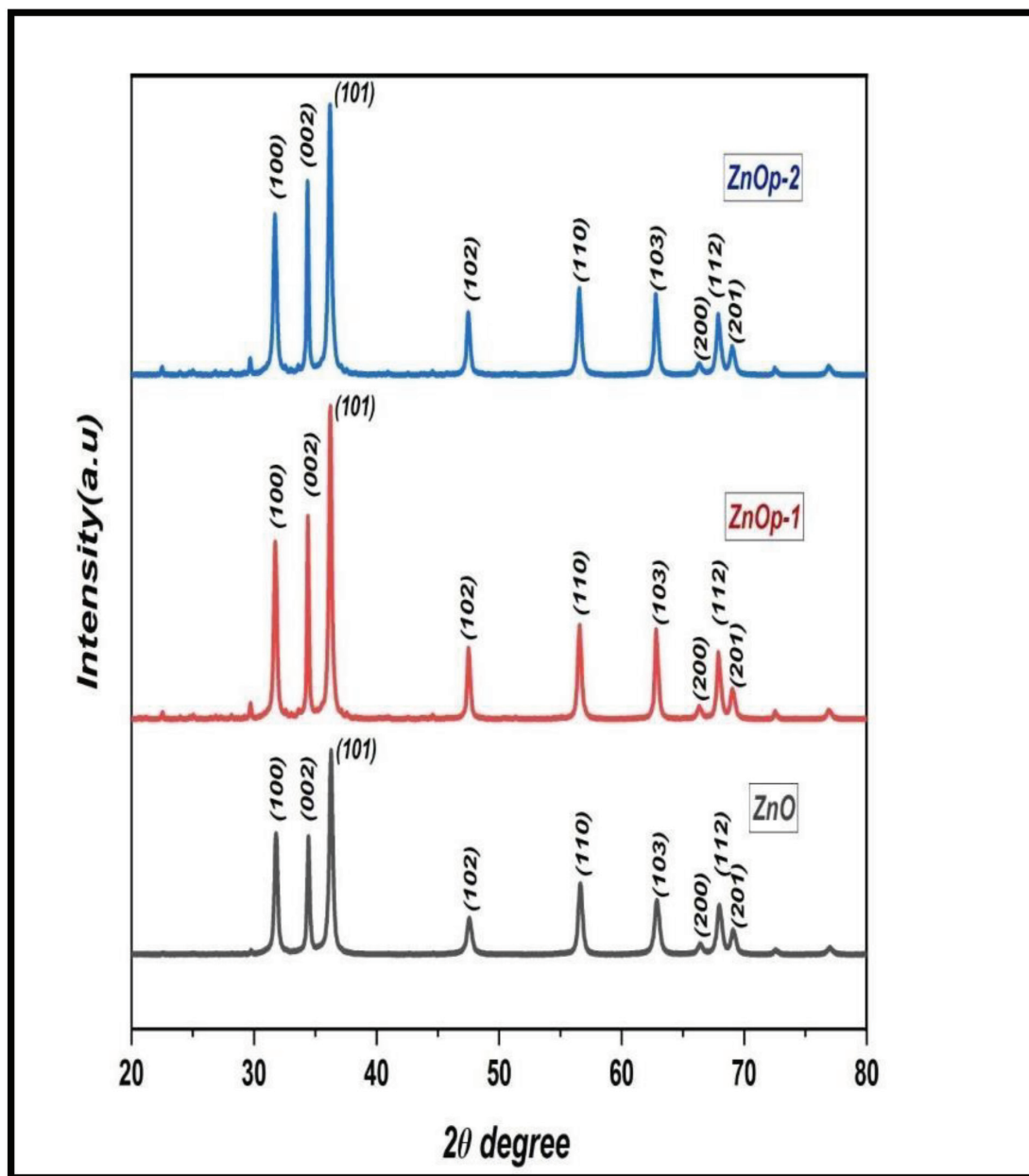


Figure 2. XRD analysis of ZnO, ZnOp-1, ZnOp-2 nanoparticles.

Oxygen, which confirms the presence of Zinc and Oxide. These values are specific for Zinc and Oxygen, which confirms the elemental composition of the compound synthesized²¹

3.5 Photoluminescence Activity

The Photoluminescence (PL) spectra of ZnO Np's synthesized at different concentrations of ZnO, ZnOp-1, ZnOp-2 is shown in Figure 9. The spectra exhibit strong emission band at 750, 749.09, 749.29 nm with an

excitation at 325nm. This range belongs to red emission region. The UV emission band is related to the near band edge emission from the ZnO direct band gap. The origin of the band between 720-780 nm. Some authors have attributed it to defects in the ZnO while some authors have suggested that such emission is a second order feature of UV emission. The emissions are generally assigned to the transition between photo-generated holes and singly ionized oxygen vacancies. Surface states are also a factor which may seriously influence the PL properties in Nanomaterials due to their large surface-to-volume ratios.

Also, surface dislocations are another factor which might play a role in the intense visible emission for the NP's. The emissions are due to Oxygen-vacancy, Zn- vacancies, interstitial zinc, contributor acceptor pairs, and surfaces states²²⁻²⁴.

3.6 UV Analysis

The valuation of the optical characteristics of ZnO nanoparticles, which were synthesized at different concentrations, elaborate an investigation of their

Table 1. Functional groups involved in ZnO nanoparticles

Wave number (cm ⁻¹) ZnO	ZnOp-1	ZnOp-2	Bond stretching
2895.80	2889.30	2880.56	C-H Stretching
2804.49	2810.98	2812.24	C-H Stretching
1647.07	1653.28	1647.28	C=C Stretching
1553.35	1554.93	1553.45	C=C Bending
1417.80	1414.17	1413.82	O=H Bending
979.70	1014.70	1022.33	C=C Bending, C-F Stretching
555.86	559.29	556.53	ZnO stretching

absorption spectra. It was observed that the plant extract served a dual purpose, functioning not only as a reducing agent but also as a stabilizing agent. This dual role was substantiated through UV-visible spectrum analysis spanning the range of 200 to 800 nm.

Figure 10 shows the absorbance spectra of ZnO nanoparticles prepared at different ratios of using *Plectranthus amboinicus* leaf extract. The optical band gap energy (Eg) is calculated using the Tauc's plot is given by

$$(\alpha h\nu) = A (h\nu - E_g)^n \quad (1)$$

Where 'A' is a photonic energy independent constant, 'h' is the Planck constant

'v' is the frequency of the photon 'α' is the absorption coefficient.

The value of 'n' is depending upon the type of transition, with 'n' equating 1/2 for indirect transitions and 2 for direct transitions. In Figure 11, the determination of energy gap values involved extrapolating lines on a graphical representation of (αhν) raised to the power 'n', intersecting with the phonon energy hν. The band gap of the pristine ZnO material was found to be 3.32 eV. As the concentration of *Plectranthus amboinicus* leaf extract increased, a corresponding increase in the band gap was observed, resulting in values of 3.31 eV and 2.29

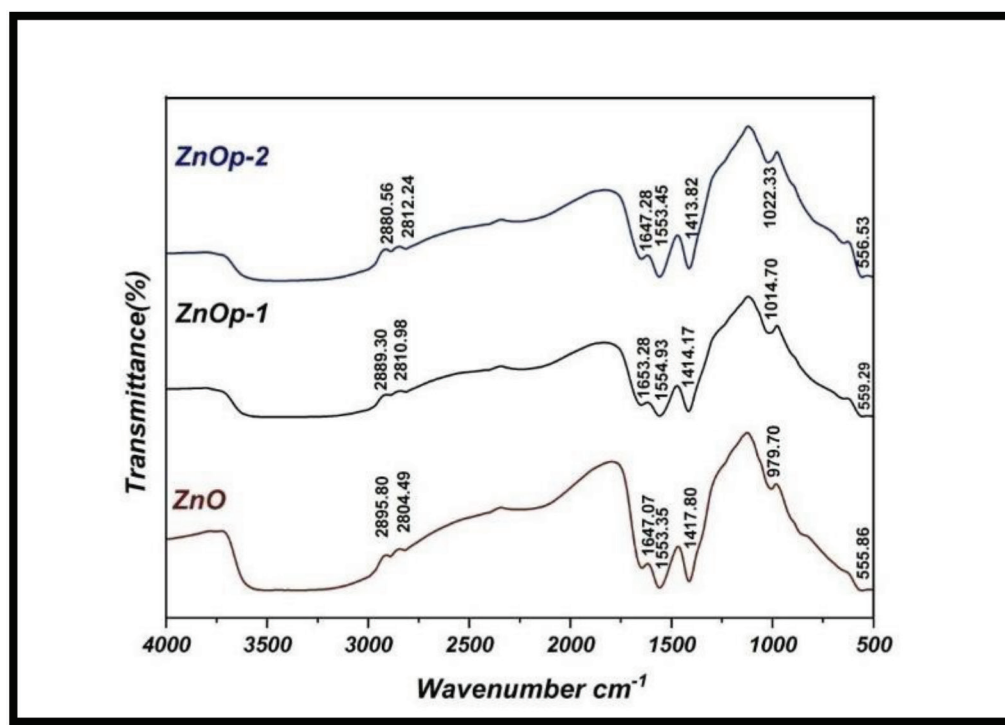


Figure 3. FTIR analysis of ZnO and green synthesized ZnO Nano particles.

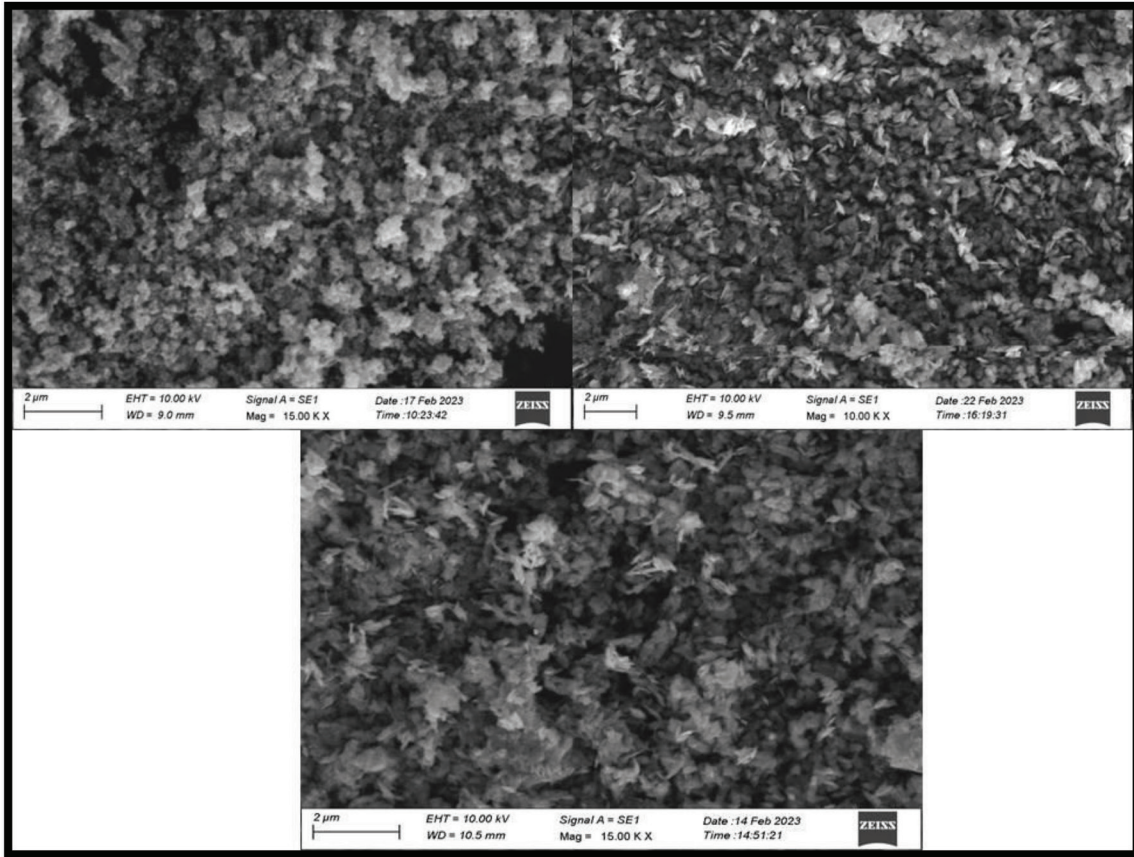


Figure 4. SEM images of ZnO, ZnOp-1, and ZnOp-2.

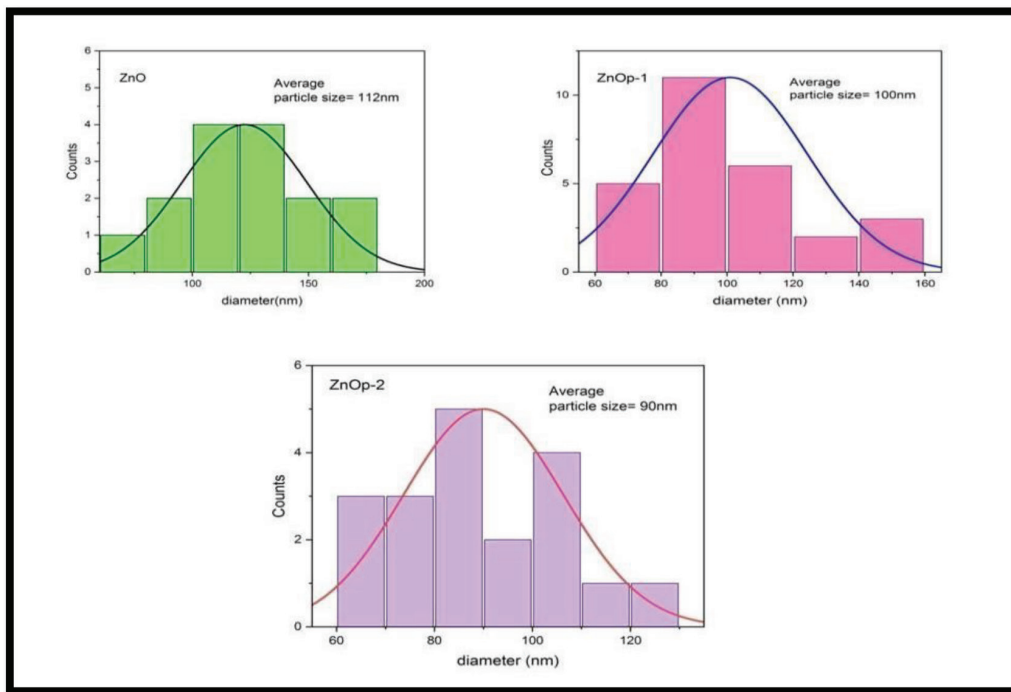


Figure 5. Particle size of ZnO, ZnOp-1, ZnOp-2.

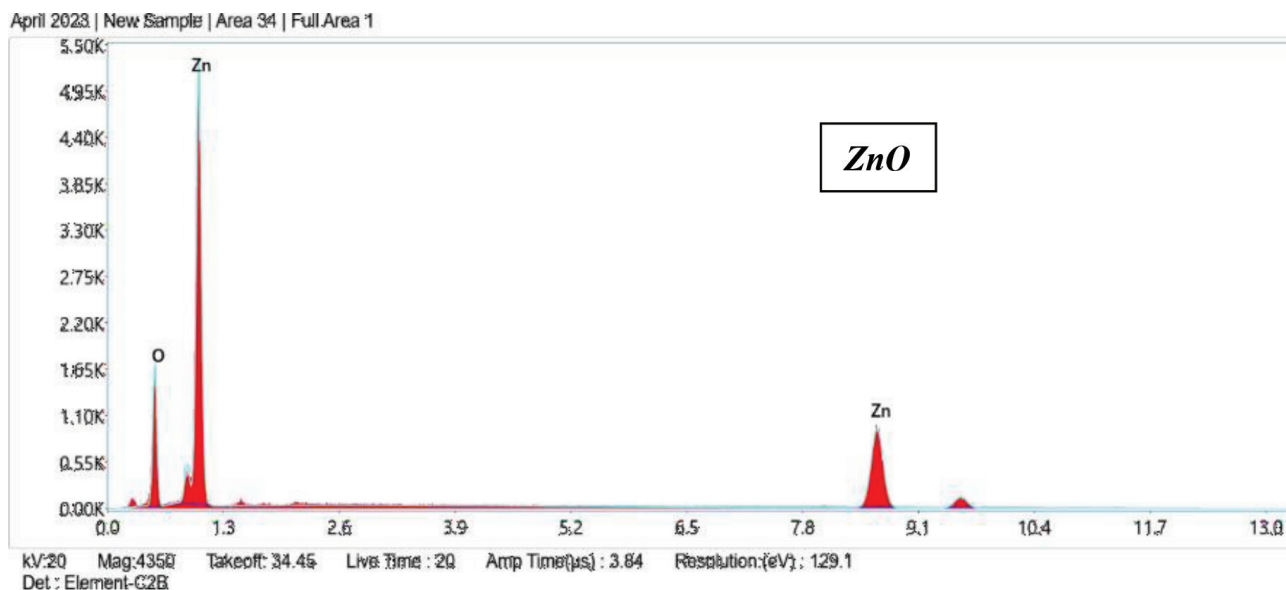
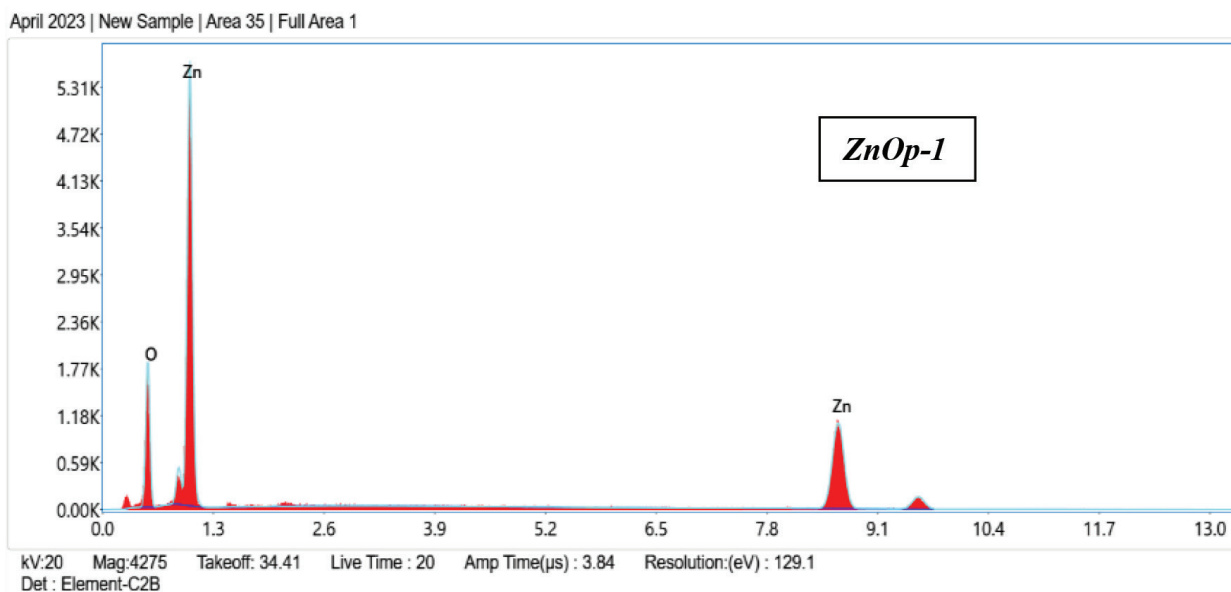
Table 2. Weight%, Atomic% for ZnO Np's

SAMPLES	ELEMENT	WEIGHT %	ATOMIC %
ZnO	Zn	73.39	40.30
	O	26.61	59.70
ZnOp-1	Zn	74.19	41.30
	O	25.81	58.70
ZnOp-2	Zn	50.69	18.90
	O	28.23	43.01

eV for ZnOp-1 and ZnOp-2, respectively (as illustrated in Figure 10). Notably, our research suggests an inverse relationship between particle size and band gap; as particle size decreased to a range of 90-112 nm, the band gap along with decreased to 2.29 eV²⁵.

3.7 Photocatalytic Effect

In Figure 12, we observe the absorption spectra depicting the degradation of MB under UV light in the presence of

**Figure 6.** EDX analysis of ZnO.**Figure 7.** EDX analysis of ZnOp-1.

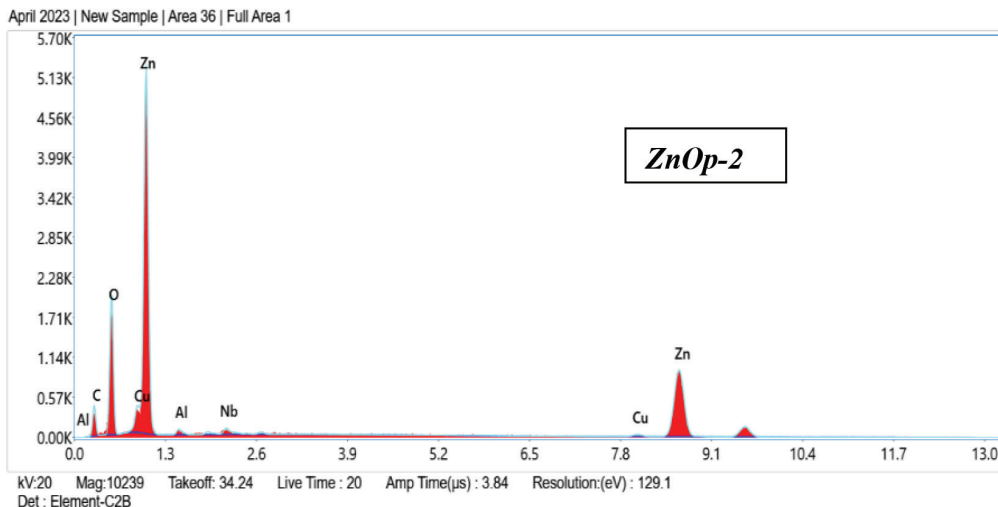


Figure 8. EDX analysis of ZnOp-2.

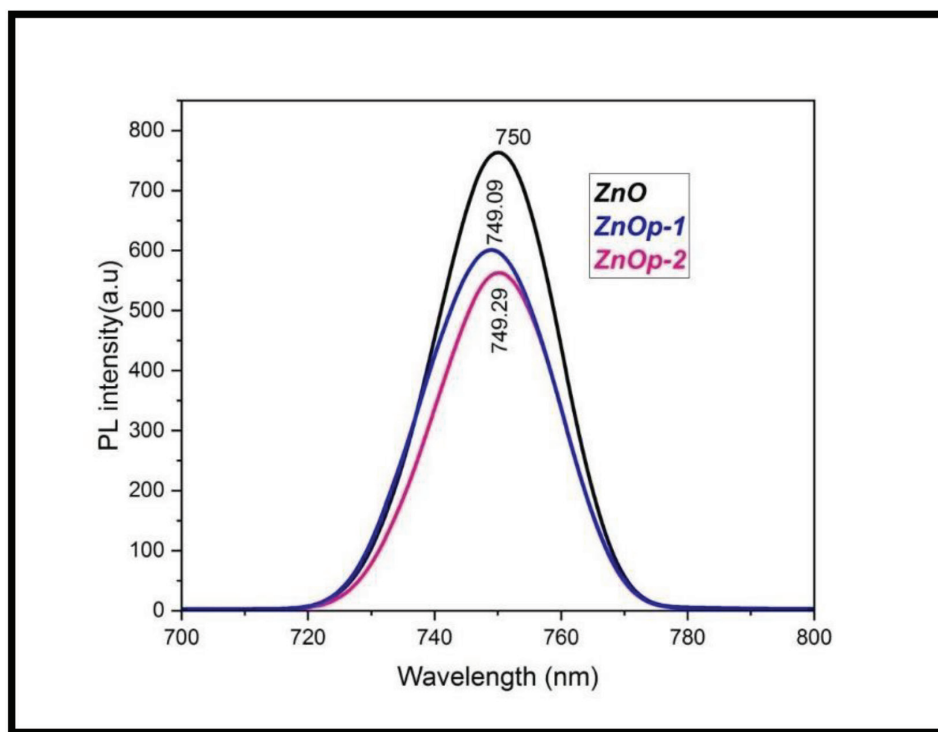


Figure 9. PL Spectra of ZnO, ZnOp-1, ZnOp-2.

ZnO nanoparticles. The reduction in absorbance intensity at 663.5 nm provides clear evidence that ZnO nanoparticles serve as effective photocatalysts for dye degradation. Particularly, ZnO nanoparticles synthesized at higher temperatures demonstrate superior removal efficiencies. The figure illustrates that the highest degradation efficiency can be achieved with ZnO, ZnOp-1, and ZnOp-2 (approximately 90% within 60 minutes). It is well-established that the

morphology, surface area, and crystalline structure of a material play pivotal roles in its photocatalytic activity. As we enhance the material's surface area and crystallinity, its photocatalytic activity improves. However, that as the material's crystallinity increases, the surface area decreases due to elevated calcination temperatures. Consequently, morphology emerges as a critical factor strongly influencing the ultimate degradation efficiency.

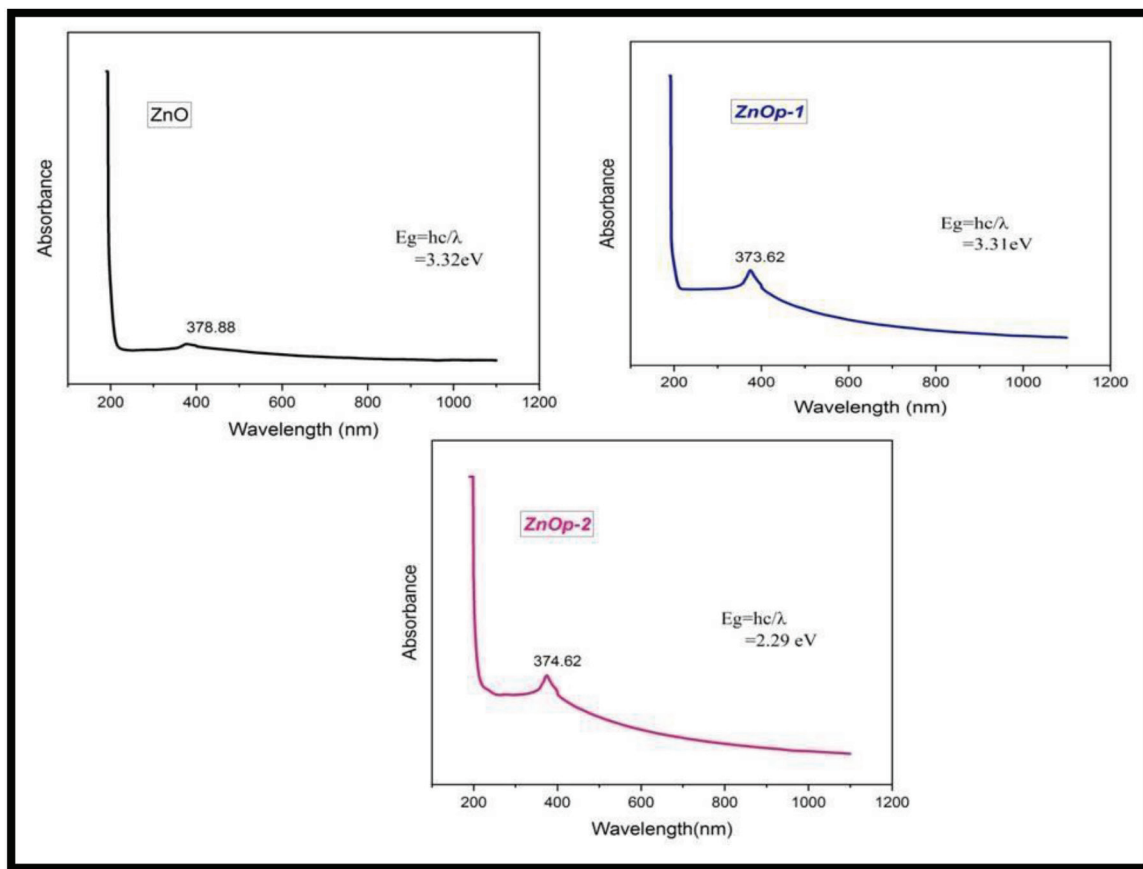


Figure 10. UV band gap energy of ZnO, ZnOp-1, ZnOp-2 nanoparticles.

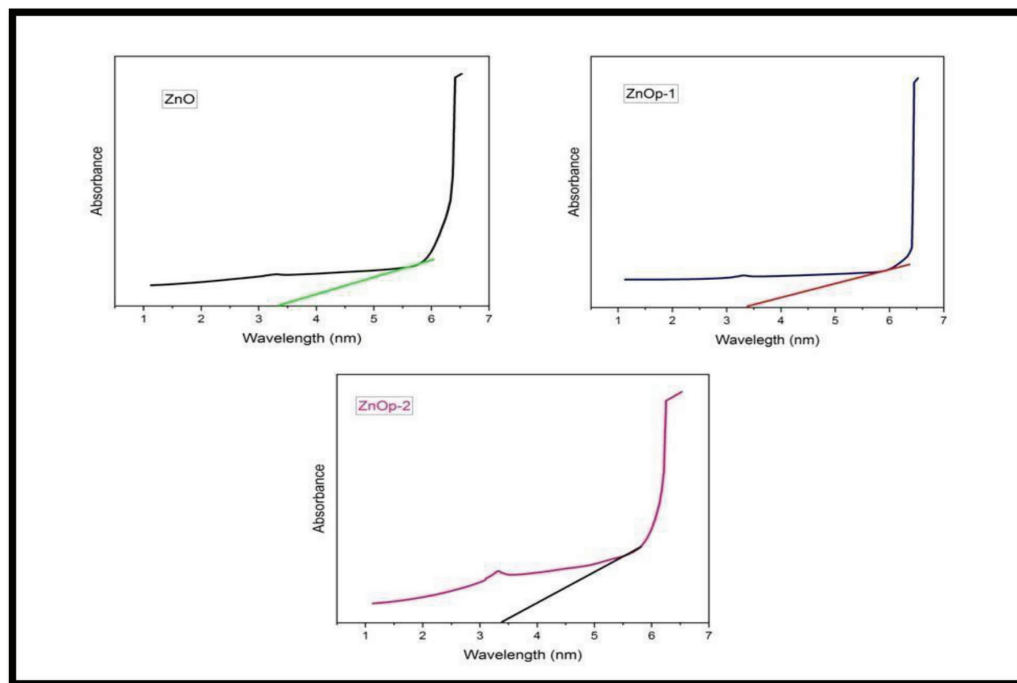


Figure 11. UV analysis of ZnO nanoparticles.

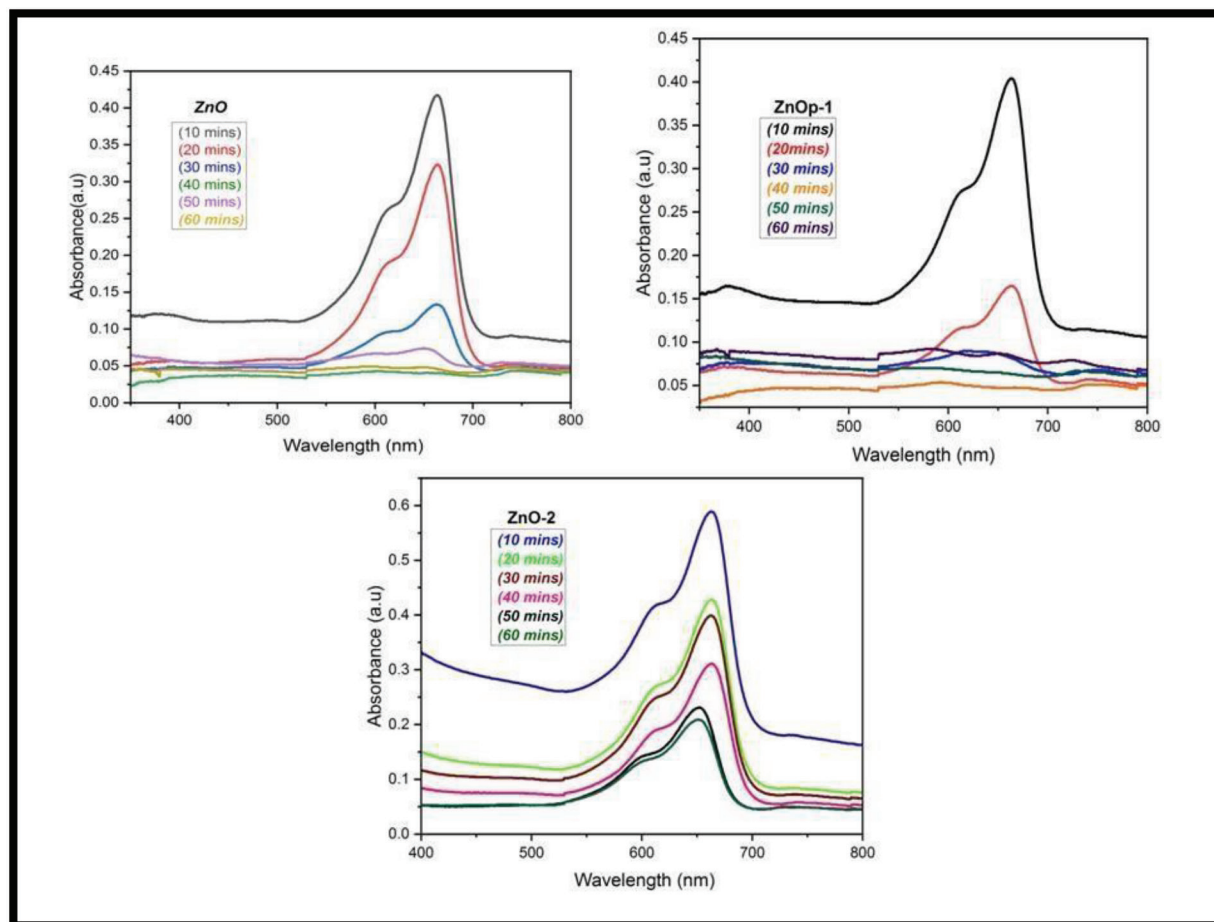


Figure 12. Photocatalytic analysis of ZnO, ZnOp-1, ZnOp-2.

4. Conclusion

In this study, we synthesized ZnO nanoparticles using the co-precipitation method at varying concentrations, employing *Plectranthus amboinicus* leaf extract as a substantial component. The X-ray diffraction (XRD) analysis confirmed the formation of ZnO nanoparticles, with crystalline sizes ranging from 32 nm to 27 nm. The Scanning Electron Microscopy (SEM) images revealed a consistent spherical morphology for pure ZnO nanoparticles. However, as the concentration of *Plectranthus amboinicus* leaf extract increased, the shape of the ZnO nanoparticles distributed uniformly without agglomeration. Energy-dispersive X-ray spectroscopy (EDX) highlighted the presence of zinc (Zn) and oxygen (O) elements. Based on UV absorption measurements, we observed a decrease in the band gap energy from 3.32 eV to 2.29 eV with increasing concentration. The Fourier-Transform Infrared (FTIR) band spectrum of ZnO nanoparticles displayed peaks at approximately 559 cm^{-1} .

Remarkably, the green-synthesized ZnO nanoparticles exhibited superior photocatalytic performance compared to pure ZnO nanoparticles. Furthermore, the photoluminescence (PL) spectra of ZnO nanoparticles displayed a prominent peak at approximately 750 nm.

5. References

1. Elishakoff I, Pentaras D, Dujat K, Versaci C, Muscolino G, Storch J, Bucas S, Challamel N, Natsuki T, Zhang YY, Wang CM, Ghyselinck G. Carbon nanotubes and nano sensors: vibrations, buckling, and ballistic impact. ISTE-Wiley. London. 2012; 13:421. <https://doi.org/10.1002/9781118562000>.
2. Vert M, Doi Y, Hellwich, KH, Hess M, Hodge P, Kubisa P, Rinaudo M, Schué FO. Terminology for biorelated polymers and applications (IUPAC Recommendations 2012). Pure and Applied Chemistry. 2012; 84(2):377-410. <https://doi.org/10.1351/PAC-REC-10-12-04>.
3. Portela Carlos M, Vidyasagar A, Krödel S, Weissenbach T, Yee Daryl W, Greer Julia R, Kochmann Dennis M. Extreme

- mechanical resilience of self - assembled nanolabyrinthine materials. *Proceedings of the National Academy of Sciences*. 2020; 117(11):5686–93. <https://doi.org/10.1073/pnas.1916817117>.
4. Medeiros PV, Marks S, Wynn JM, Vasylenko A, Ramasse QM, Quigley D, Sloan J, Morris AJ. Single-atom scale structural selectivity in Te nanowires encapsulated inside Ultranarrow, single-walled carbon nanotubes. *ACS Nano*. 2017; 11(6):6178–85. <https://doi.org/10.1021/acsnano.7b02225>.
 5. Pervez Md N, Balakrishnan M, Hasan SW, Choo K-H, Zhao Y, Cai Y, Zarra T, Belgiorno V, Naddeo V. A critical review on nanomaterials membrane bioreactor (NMs-MBR) for wastewater treatment. 2020. <https://doi.org/10.1038/s41545-020-00090-2>.
 6. Gleason Karen K, Kenneth KSL, Jeffrey AC. Structure and morphology of fluorocarbon films grown by hot filament chemical vapor deposition. *Chemistry of Materials*. 2000; 12(10):3032. <https://doi.org/10.1021/cm000499w>.
 7. Gour A, Narendra KJ. Advances in green synthesis of nanoparticles. *Artificial Cells, nanomedicine, and biotechnology*. 2019; 47(1):844-51. <https://doi.org/10.1080/21691401.2019.1577878>.
 8. *Plectranthus amboinicus* (Indian borage), Datasheet, Invasive Species Compendium. Centre for Agriculture and Biosciences International. 2017.
 9. Ahmad W, Divya K. Green synthesis, characterization and anti-microbial activities of ZnO nanoparticles using *Euphorbia hirta* leaf extract. *Journal of King Saud University-Science*. 2020; 32(4):2358-64. <https://doi.org/10.1016/j.jksus.2020.03.014>.
 10. Vinotha V, *et al.* Synthesis of ZnO nanoparticles using *insulin-rich* leaf extract: Anti-diabetic, antibiofilm and antioxidant properties. *Journal of Photochemistry and Photobiology B: Biology*. 2019; 197:111541. <https://doi.org/10.1016/j.jphotohiol.2019.111541>.
 11. Vijayakumar S, *et al.* *Acalypha fruticosa* L. leaf extract mediated synthesis of ZnO nanoparticles: Characterization and antimicrobial activities. *Materials Today: Proceedings*. 2020; 23:73-80. <https://doi.org/10.1016/j.matpr.2019.06.660>.
 12. Subbiah R, Muthukumaran S, Raja V. Biosynthesis, structural, photoluminescence and photocatalytic performance of Mn/Mg dual doped ZnO nanostructures using *Ocimum tenuiflorum* leaf extract. *Optik*. 2020; 208:164556. <https://doi.org/10.1016/j.ijleo.2020.164556>.
 13. Kumar KS, Dhananjaya N, Yadav LR. *E. tirucalli* plant latex mediated green combustion synthesis of ZnO nanoparticles: Structure, photoluminescence and photocatalytic activities. *Journal of Science: Advanced Materials and Devices*. 2018; 3(3):303-9. <https://doi.org/10.1016/j.jsamd.2018.07.005>.
 14. Anbuvaran M, *et al.* *Vitex negundo* leaf extract mediated synthesis of ZnO nanoplates and its antibacterial and photocatalytic activities. *Asian Journal of Nanoscience and Materials*. 2019; 2:99-110.
 15. Nithya K, Kalyanasundharam S. Effect of chemically synthesis compared to biosynthesized ZnO nanoparticles using aqueous extract of *C. halicacabum* and their antibacterial activity. *Open Nano*. 2019; 4:100024. <https://doi.org/10.1016/j.onano.2018.10.001>.
 16. Rafique M, *et al.* Novel, facile and first time synthesis of zinc oxide nanoparticles using leaves extract of *Citrus reticulata* for photocatalytic and antibacterial activity. *Optik*. 2021; 243:167495. <https://doi.org/10.1016/j.ijleo.2021.167495>.
 17. Abbas Q. Understanding the UV-Vis spectroscopy for nanoparticles. *J Nanomater Mol Nanotechnol*. 2019; 8:3.
 18. Stokes DJ. Principles and practice of variable pressure environmental scanning electron microscopy (VP-ESEM). Chichester: John Wiley and Sons. 2008. <https://doi.org/10.1002/9780470758731>.
 19. Osasih FU, Cacovich S, Divitini G, Ducati C. Nanometric chemical analysis of beam-sensitive materials: a case study of stem-edx on perovskite solar cells. 2020. <https://doi.org/10.1002/smt.202000835>.
 20. Coronado JM, Fresno F, Hernández-Alonso MD, Portela R. Design of advanced photocatalytic materials for energy and environmental applications. London: Springer. 2013; 1–5. <https://doi.org/10.1007/978-1-4471-5061-9>.
 21. Tebyetekerwa M, Zhang J, Xu Z, Truong TN, Yin Z, Lu Y, Ramakrishna S, Macdonald D, Nguyen HT. mechanisms and applications of steady-state photoluminescence spectroscopy in two-dimensional transition-metal dichalcogenides. *ACS Nano*. 2020; 14(11):14579–604.
 22. Prasad N, Basalingappa K, Razvi S, Murugesan K. Nutritional significance of Indian borage (*Plectranthus Amboinicus*): a review. *Plant Archives*. 2020; 20:3727-30.
 23. Patel R, Naveen M, Manjul PS, Alam DR, Anita S, Singh S. *Plectranthus amboinicus* (Lour) Spreng: an overview. *The Pharma Research*. 2010; 4:1-15.
 24. Chandrasekar LP, Sethuraman BD, Subramani M, Mohandos S. Green synthesised ZnO nanoparticles from *Plectranthus amboinicus* plant extract: removal of Safranin- O and Malachite green dyes and anti-bacterial activity. *International Journal of Environmental Analytical Chemistry*. 2023. <https://doi.org/10.1080/03067319.2023.2190458>.
 25. Ganapathy NRV, Krishnan V, Veeraraghavan AJ, Varatharajan, Devaraj G. Biosynthesis of zinc oxide nanoparticles from *Plectranthus amboinicus* and its photocatalytic effect on wastewater treatment. *International Journal of Recent Technology and Engineering (IJRTE)*. 2019; 8(4S2). <https://doi.org/10.35940/ijrte.D1140.1284S219>.
 26. Nguyen NT, Nguyen VA. Synthesis, characterization, and photocatalytic activity of ZnO nanomaterials prepared by a green, nonchemical route. *Hindawi Journal of Nanomaterials*. 2020; 8. <https://doi.org/10.1155/2020/1768371>.